Article

Mapping Proteolytic Processing in the Secretome of Gastric Cancer-Associated Myofibroblasts Reveals Activation of MMP-1, MMP-2, and MMP-3

Christopher Holmberg,[†] Bart Ghesquière,[‡,§] Francis Impens,[‡,§] Kris Gevaert,[‡,§] J. Dinesh Kumar,[†] Nicole Cash,[†] Sandhir Kandola,[†] Peter Hegyi,[‖] Timothy C. Wang,[#] Graham J. Dockray,[†] and Andrea Varro*,[†]

[†]Institute of Translational Medicine, University of Liverpool, Liverpool, U.K.

[‡]Department of Medical Protein Research, VIB, Ghent, Belgium

[§]Department of Biochemistry, Ghent University, Ghent, Belgium

[‖]First Department of Medicine, University of Szeged, Szeged, Hungary

[#]Department of Medicine, Columbia University Medical Center, New York, United States

S *Supporting Information*

ABSTRACT: Cancer progression involves changes in extracellular proteolysis, but the contribution of stromal cell secretomes to the cancer degradome remains uncertain. We have now defined the secretome of a specific stromal cell type, the myofibroblast, in gastric cancer and its modification by proteolysis. SILAC labeling and COFRADIC isolation of methionine containing peptides allowed us to quantify differences in gastric cancer-derived myofibroblasts compared with myofibroblasts from adjacent tissue, revealing increased abundance of several proteases in cancer myofibroblasts including matrix metalloproteinases (MMP)-1 and -3. Moreover, N-terminal COFRADIC analysis identified cancer-restricted proteolytic cleavages, including liberation of the active forms of MMP-1, -2, and -3 from their inactive precursors. In vivo imaging confirmed increased MMP activity when gastric cancer cells were xenografted in mice together with gastric cancer myofibroblasts. Western blot and enzyme activity assays confirmed increased MMP-1, -2, and -3 activity in cancer myofibroblasts, and cancer cell migration assays indicated stimulation by MMP-1, -2, and -3 in cancer-associated myofibroblast media. Thus, cancer-derived myofibroblasts differ from their normal counterparts by increased production and activation of MMP-1, -2, and -3, and this may contribute to the remodelling of the cancer cell microenvironment.

KEYWORDS: *myofibroblast, secretome, COFRADIC, degradome, neo-N-termini*
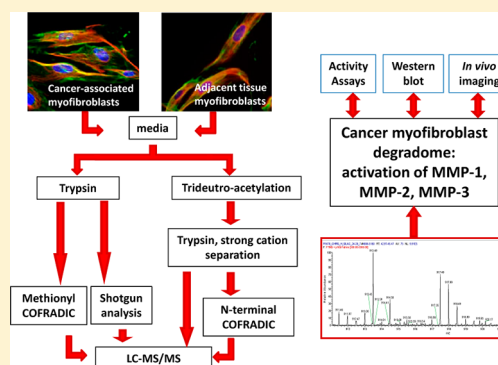
INTRODUCTION

Elucidation of the dynamic changes in secretomes, i.e., the secreted subset of the proteome, underlies a systems approach to understanding the mechanisms controlling cell–cell and cell–matrix interactions in health and disease. In cancer it is now clear that changes in the cellular microenvironment determine disease progression, and that these include two-way interactions between cancer cells and surrounding stromal cells.[1–3]

Several recent studies have employed proteomic techniques to define the secretomes of cancer cells.[4–10] Recent studies have also defined the secretome in breast and colon cancer fibroblasts,[11,12] but in general the interrogation of stromal cell secretomes by proteomic methods has been limited. Changes in secretomes may reflect alterations in secretory protein abundance due to variations in gene expression, rates of exocytosis or presecretory post-translational processing. But in addition, there may also be extensive postsecretory proteolysis

that defines the extracellular tumor degradome. In cancer, alterations in extracellular proteolysis through differential secretion of proteases or their inhibitors is important, not least because it underlies disease progression and sensitivity to protease targeted therapies.[13–15]

Cancer-associated fibroblasts, of which myofibroblasts are a subset, are important stromal cells that exhibit an altered phenotype in many cancers.[16–19] Myofibroblasts play important roles in defining the tissue microenvironment through secretion of extracellular matrix components, growth factors, proteases and their inhibitors.[20,21] Differences between normal and cancer-associated myofibroblasts (CAMs) have been linked to tumor progression by mechanisms including recruitment from circulating mesenchymal stromal cells, global DNA hypomethylation and changes in gene expression profiles.[22–24]

Since myofibroblasts stimulate cancer cell invasion, in the present study we sought to define the differences between gastric CAMs compared with adjacent tissue-derived myofibroblasts (ATMs) with respect to proteolytic processing of their secretomes. The data indicate both upregulation and activation of matrix metalloproteinases (MMPs)-1, -2, and -3 are characteristic of the CAM secretome.

■ MATERIALS AND METHODS

Human Primary Myofibroblasts

Myofibroblasts from gastric cancers (CAMs) and adjacent tissue (ATMs) from two patients have been described previously (Supporting Information).[19] The work was approved by the Ethics Committee of the University of Szeged, Hungary, and subjects provided informed consent.

SILAC Labeling

Myofibroblasts were cultured in DMEM SILAC media (Pierce, Thermo Scientific, Rockford, IL, USA) for 6 population doublings in the presence of either natural (light) or heavy $^{13}C_6$-labeled L-arginine (0.94 mM) and $^{13}C_6$ L-lysine (0.46 mM) (Invitrogen, Paisley, Renfrew, U.K.). Media were further supplemented with 10% dialyzed fetal bovine serum (Pierce), 2% antibiotic/antimycotic (Sigma-Aldrich, Poole, U.K.) and 1% penicillin/streptomycin (Sigma).

Sample Preparation

Media (10 mL, serum-free) obtained from 1×10^6 myofibroblasts plated in 10 cm diameter dishes (80−90% confluency) were collected after 24 h. Samples were concentrated to approximately 0.5 mL using Amicon Ultra-15 3 kDa centrifugal filter devices (Millipore, Watford, U.K.), precipitated with 20% TCA and resuspended in 50 mM HEPES, pH 7.4, 100 mM NaCl, 0.8% w/v CHAPS, 1% v/v Protease Inhibitor Cocktail Set III, EDTA-Free (Calbiochem, Merck Biosciences, Beeston, U.K.). Equal amounts (35 μg each) of light and heavy SILAC-labeled secretome samples from CAMs and ATMs were mixed following determination of protein concentration by the Bradford assay (Bio-Rad Lab, Inc., Hemel Hempstead, U.K.).

COFRADIC Isolation of Methionine Containing Peptides

Methionyl-COFRADIC was performed as described previously[25] (see Supporting Information Methods). Samples were reduced and S-alkylated, and following trypsinization (trypsin:protein 1:100), peptides were fractionated by reversed-phase HPLC (RP-HPLC) using an Agilent 1100 HPLC system with a Zorbax 300SB-C_{18} column (2.1 mm (internal diameter) × 150 mm, Agilent Technologies, Wokingham, U.K.). The resulting HPLC fractions were further processed by incubating for 30 min with 0.1% w/v hydrogen peroxide at 30 °C. Following oxidation of methionines, reaction mixtures were immediately reinjected onto the RP-HPLC column for secondary RP-HPLC separations under identical conditions. Fractions with methionine containing peptides displayed a hydrophilic shift and were collected (n = 90) and analyzed by LC−MS/MS.

COFRADIC Isolation of N-Terminal Peptides

N-terminal COFRADIC was performed as described previously[26,27] (see Supporting Information Methods). Proteins were reduced and alkylated, and primary α- and ε-amines were blocked by trideutero-acetylation. Samples were then trypsinized, and N-terminal peptides were pre-enriched by strong cation exchange chromatography at low pH. Following a pyro-glutamate removal step, peptides were separated by RP-HPLC as described above. Primary fractions were incubated with 2,4,6-trinitrobenzenesulphonic acid (TNBS) to modify internal tryptic peptides with free α-N-termini. A series of secondary RP-HPLC runs was then performed on each individual primary fraction, and N-terminal peptides (which did not display a hydrophobic shift) were collected (n = 36) for LC−MS/MS analysis.

Non-COFRADIC Experiments

Samples prepared for "shotgun" analysis of the secretomes were processed following the same method as for Met-COFRADIC up to the stage immediately before the first RP-HPLC run. At this point the sample was processed for LC−MS/MS analysis (see Supporting Information Methods).

For neo-N-terminal enrichment, the non-COFRADIC method employed a SCX-only enrichment of N-terminal peptides. Samples were prepared as for N-terminal COFRADIC up to the first RP-HPLC run. At this stage 60 fractions of 1 min interval were collected, pooled to give a total of 20 fractions, dried and prepared for LC−MS/MS analysis.

LC−MS/MS Analysis and Peptide Identification by Mascot

Peptides were analyzed using a LTQ Orbitrap XL mass spectrometer (Thermo Electron, Bremen, Germany) as described previously.[28] Mascot generic files (mgf) were created using the Mascot Distiller software (version 2.2.1.0, Matrix Science, Ltd., London, U.K.). When generating peak lists, grouping of spectra was performed with a maximum intermediate retention time of 30 s and maximum intermediate scan count of 5. Grouping was further done with 0.1 Da precursor ion tolerance. A peak list was only generated when the spectrum contained more than 10 peaks. There was no deisotoping, and the relative signal-to-noise limit for both precursor and fragment ions was set to 2. The peak lists were then searched with Mascot using the Mascot Daemon interface (version 2.2.0, Matrix Science, Ltd.) against human proteins in the Swiss-Prot database (Uniprot release 15.0, containing 20 333 human protein sequences). Spectra were searched with semiArgC/P enzyme settings, allowing no missed cleavages for the N-terminal peptide experiments, and with trypsin/P settings allowing no missed cleavages for the Met-COFRADIC/shotgun experiments. Mass tolerance of the precursor ions was set to 10 ppm (with Mascot's C13 option set to 1) and of fragment ions to 0.5 Da. The instrument setting was ESI-TRAP. Variable modifications were acetylation of alpha-N-termini and pyroglutamate formation of N-terminal glutamine residues; fixed modification was oxidation of methionine (sulfoxide). Additionally, for N-terminal peptide experiments, trideutero-acetylation of the N-terminus was set as variable peptide modification, and trideutero-acetylation of lysine side chains was included as fixed modification. Only peptides that were ranked one and scored above the identity threshold score set at 99% confidence were withheld. The FDR was calculated for every search as described previously (see Supporting Information Methods, Table SM3).[28] Identified peptides were quantified using the Mascot Distiller Quantitation Toolbox (www.matrixscience.com) in the "precursor" mode as described previously.[29] Ratios for all peptides of interest were validated by manual inspection of spectra. For processing of all MS data, the ms_lims software platform was used.[30] Protein ratios were inferred using the mean of the peptide group ratios for each protein. A peptide group represents all quantifications of a single peptide sequence in an experiment. The distribution of
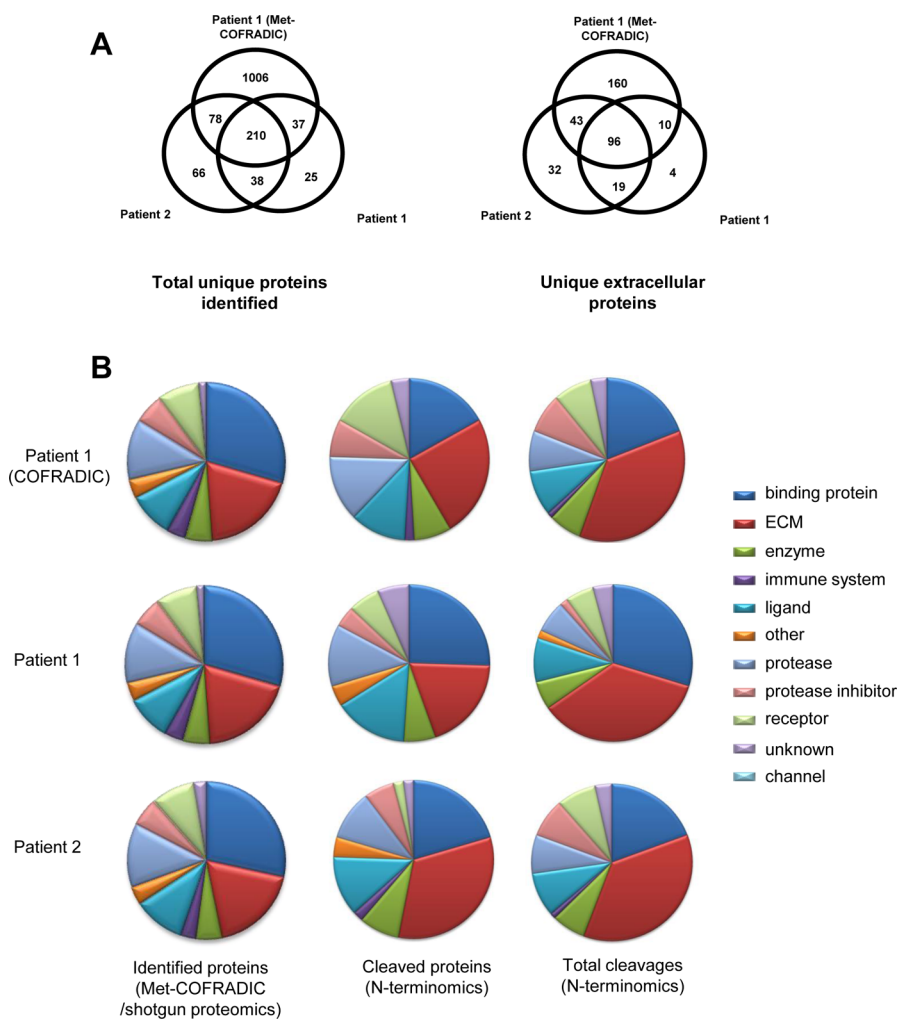
Figure 1. Myofibroblast secretomes. (A) Venn diagram showing, left, identification of unique proteins, on the basis of one or more unique peptides with a validated quantification, in media from pairs of CAMs/ATMs from two patients, and overlap with Met-COFRADIC identifications in patient 1 based on the same criteria; right, extracellular proteins in this data set. (B) Functional classification of extracellular proteins identified by Met-COFRADIC and classical "shotgun" proteomics, alongside cleaved proteins and total cleavage products in myofibroblast secretomes by N-terminal peptide enrichment (restricted to identifications with successful quantification).

protein ratios as determined by the Met-COFRADIC and shotgun experiments was plotted using Rover.[31] This was used to define thresholds to give the 5% of proteins with the largest fold changes in CAMs relative to ATMs. All spectra have been stored in the PRIDE database (http://www.ebi.ac.uk/pride/, accession numbers 27157−27161) using PRIDE converter.[32] Protein subcellular localizations and functional classifications were manually curated, using the UniProt and HPRD online databases.

In Vivo Imaging

Immunocompromised mice (6 weeks old, BALB/c nu/nu, Charles River, Wilmington, MA) with xenogafts of MKN45 cells with or without CAMs (Supporting Information Methods) were used for imaging MMP-activity using MMPSense 750 FAST. These experiments were approved by the University of Liverpool Animal Welfare Committee and were conducted in compliance with the U.K. Animals (Scientific Procedures) Act 1986.

Western Blot

Myofibroblast cell extracts were prepared in RIPA buffer containing protease and phosphatase inhibitors. Cell extracts or

media were resolved by SDS-PAGE and processed for Western blotting as previously described.[33] Blots were probed with antibodies against MMP-1 (BAF901, R&D Systems, Minneapolis, MN, USA), MMP-2 (BAF902, R&D Systems) and MMP-3 (BAF513, R&D Systems). Membranes were reprobed with anti-GAPDH antibody (Biodesign, Saco, Maine, USA) for assessing equal loading where appropriate.

Enzyme Assays

Fluorogenic assays for MMP enzyme activity were performed using selective substrates: DNP-Pro-Leu-Ala-Leu-Trp-Ala-Arg-OH (MMP-1; Calbiochem, Bedfont Cross, U.K.), DNP-Pro-Leu-Gly-Met-Trp-Ser-Arg-OH (MMP-2/9; Calbiochem), MCA-Pro-Leu-Ala-Nva-Dpa-Ala-Arg-NH$_2$ (MMP-2; Calbiochem), DNP-Pro-Tyr-Ala-Ty-Trp-Met-Arg-OH (MMP-3; AnaSpec, Fremont, CA, USA) and 5-FAM-Arg-Pro-Lys-Pro-Val-Glu-Nva-Trp-Arg-Lys(TQ2W)-NH$_2$ (MMP-3; Enzo Life Sciences, Exeter, U.K.) as previously described.[33,34] Briefly, equal volumes of assay buffer and media from 10^5 myofibroblasts were incubated with 12 μM substrate as appropriate.

Table 1. Neo-N-terminal Peptides of Extracellular Proteins Unique to CAMs (i.e., Singletons), Excluding Those Representing Removal of a Signal Sequence[a]

Uniprot	functional classification	description	cleavage site	start	end	peptide	patient 1	patient 2	patient 1 (N-terminal COFRADIC)[a]
P07858	protease	Cathepsin B	Cathepsin B heavy chain	321	331	IESEVVAGIPR	CAM singleton		
P14209	binding protein	CD99 antigen	Extracellular domain	89	115	SFSDADLADGVSGGEGKGGSDGGGSHR	CAM singleton		
P12110	ECM	Collagen alpha-2(VI) chain	Nonhelical region	772	784	LYSIACDKPQQVR			CAM singleton
P30443	receptor	HLA class I histocompatibility antigen, A-1 alpha chain	Alpha-1 region	60	72	FDSDAASQKMEPR			CAM singleton
P01889	receptor	HLA class I histocompatibility antigen, B-7 alpha chain	Alpha-1 region	51	59	YVDDTQFVR			CAM singleton
P10321	receptor	HLA class I histocompatibility antigen, Cw-7 alpha chain	Alpha-1 region	32	38	FDTAVSR			CAM singleton
P03956	protease	Interstitial collagenase	Propeptide	22	49	ATLETQEQDVDLVQKYLEKYNLKNDGR		CAM singleton	
P03956			Propeptide	84	91	LKVMKQPR		CAM singleton	
P03956			Propeptide	75	91	VTGKPDAETLKVMKQPR	CAM singleton		
P22064	binding protein	Latent-transforming growth factor beta-binding protein, isoform 1S	Main chain	449	461	AKEEPVEALTFSR			CAM singleton
Q9Y4K0	enzyme	Lysyl oxidase homologue 2	SRCR1 domain	52	59	NVAKIQLR			CAM singleton
P04156	unknown	Major prion protein	Main chain	120	136	AVVGGLGGYMLGSAMSR	CAM singleton		
P04156			Main chain	138	148	IIHFGSDYEDR			CAM singleton
Q02297	ligand	Pro-neuregulin-1, membrane-bound isoform	Main chain	229	242	VQNQEKAEELYQKR			CAM singleton
P08254	protease	Stromelysin-1	Propeptide	92	101	CGVPDVGHFR			CAM singleton
P08254			Propeptide	56	65	DSGPVVKKIR	CAM singleton		
P08254			Propeptide	79	88	LDSDTLEVMR	CAM singleton		
Q9UBN6	receptor	Tumor necrosis factor receptor superfamily member 10D	TBFR-Cys 1 repeat	77	89	SLKEEECPAGSHR	CAM singleton		

[a]Functional classification and cleavage sites were manually annotated using Uniprot database. Start and end position number of the N-terminally labeled peptide are relative to unprocessed forms of the protein.
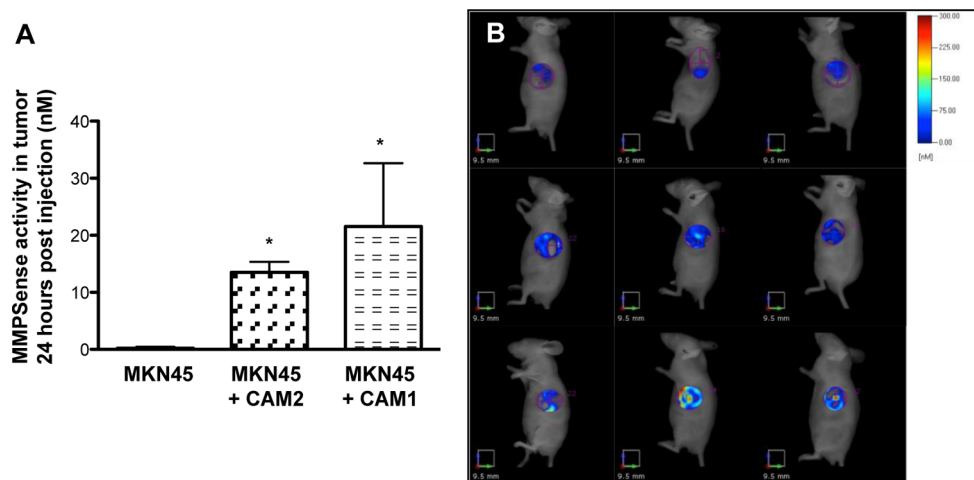
Figure 2. Increased MMP activity in vivo in xenografts containing CAMs. (A) In BALB/c nu/nu mice, MMP activity revealed by FMT imaging of MMPSense 750 FAST is increased in xenografts of gastric cancer MKN45 cells containing two different CAMs compared with MKN45 cells alone. (B) Representative FMT images of mice with xenografts of MKN45 cells alone (top row), MKN45 cells + CAM2 (middle row), and MKN45 cells + CAM1 (bottom row).

Migration Assays

Gastric cancer cell (AGS) migration (10^5 cells per 8 μm pore filter insert) (BD Biosciences, Oxford, U.K.) was studied as previously described.[35,36] Conditioned media were collected as described above and treated with MMP-1 neutralizing antibody (MAB901, R&D Systems), or selective MMP-2 (inhibitor I, Calbiochem) and MMP-3 (inhibitor IV, Calbiochem) inhibitors as appropriate.

Statistics

Results are expressed as mean $\pm$ standard error of the mean (SEM), unless otherwise stated. Student's t-test or ANOVA (Systat Software, Inc., Hounslow, London, U.K.) as appropriate were used to determine statistical significance of results and considered significant at $p < 0.05$, unless otherwise stated.

■ RESULTS

Different Secretomes in Cancer-Derived and Adjacent Tissue Myofibroblasts

When myofibroblasts derived from two gastric cancers and corresponding ATMs were SILAC labeled and the secretomes analyzed by LC–MS/MS, approximately 350 unique proteins (310 and 392) were identified in each pair on the basis of one or more peptide unique assignments with validated quantification (Supporting Information Tables S1, S2). Of these, 42 and 48% were characterized as extracellular proteins on the basis of annotations in the UniProt and HPRD databases. One of the paired samples was further analyzed using the COFRADIC technology that enriches for methionine-containing peptides in an attempt to increase overall proteome coverage by reducing sample complexity. This approach more than doubled the number of unique peptides and proteins identified in the secretome, although a comparable proportion (31%) of the identifications were attributable to extracellular proteins (Figure 1A; Supporting Information Table S3). The Met-COFRADIC analysis identified the majority (72%) of proteins identified in the initial experiments (Figure 1A). In total across the three experiments, 1460 unique proteins were identified, of which 364 were annotated to be extracellular proteins.

Extracellular proteins making up the secretome were grouped into 11 functional classifications (Figure 1B). There was a broadly similar distribution across these groups in both pairs of CAMs and ATMs, with binding proteins and extracellular matrix proteins the two largest groups (Figure 1B). When 95% confidence limits were determined and applied to individual experiments, 9–47 proteins were identified that were above or below these limits (Supporting Information Figure S1; Supporting Information Table S4). Interestingly, MMP-1, MMP-3, MMP-10 and uPA were identified as upregulated in CAMs in both patients (Supporting Information Table S4). The largest groups showing differential abundance were "binding" proteins, e.g., the insulin-like growth factor binding proteins (IGFBPs), "receptor" proteins, e.g., epidermal growth factor receptor, and proteases, e.g., MMP-1 (Supporting Information Table S4).

Proteolytic Processing of the Secretome

We then extended the analysis to the identification of neo-N-termini generated as a consequence of proteolytic cleavage. Thus, SILAC-labeled media samples were enriched for N-terminal peptides using a strong cation exchange (SCX) step to remove nonterminal peptides. As part of this procedure, neo-N-terminal peptides had been trideutero-acetylated prior to trypsinisation to facilitate discrimination from other peptides by mass spectrometry, and the results were filtered so that only peptides that were trideutero-acetylated and had a valid Mascot identification were used in subsequent analyses. Of unique quantified peptides, 20–42% were trideutero-acetylated (Supporting Information Table S5). This process identified peptides starting at residues 1 or 2 of the protein or immediately after removal of the signal sequence, which were excluded from further analysis as they were considered uninformative for present purposes. For each of the remaining peptides, the ratio of relative abundance between the CAM and ATM samples was manually validated by inspecting the spectra and calculating the area under the peaks of the heavy and light isotopes.

One of the paired samples was further analyzed using N-terminal COFRADIC in addition to the SCX enrichment step in an attempt to increase coverage of N-terminal peptides by reducing sample complexity. Similar numbers of peptides were identified by N-terminal COFRADIC and SCX-only enrichment, but over 2-fold more of these identifications
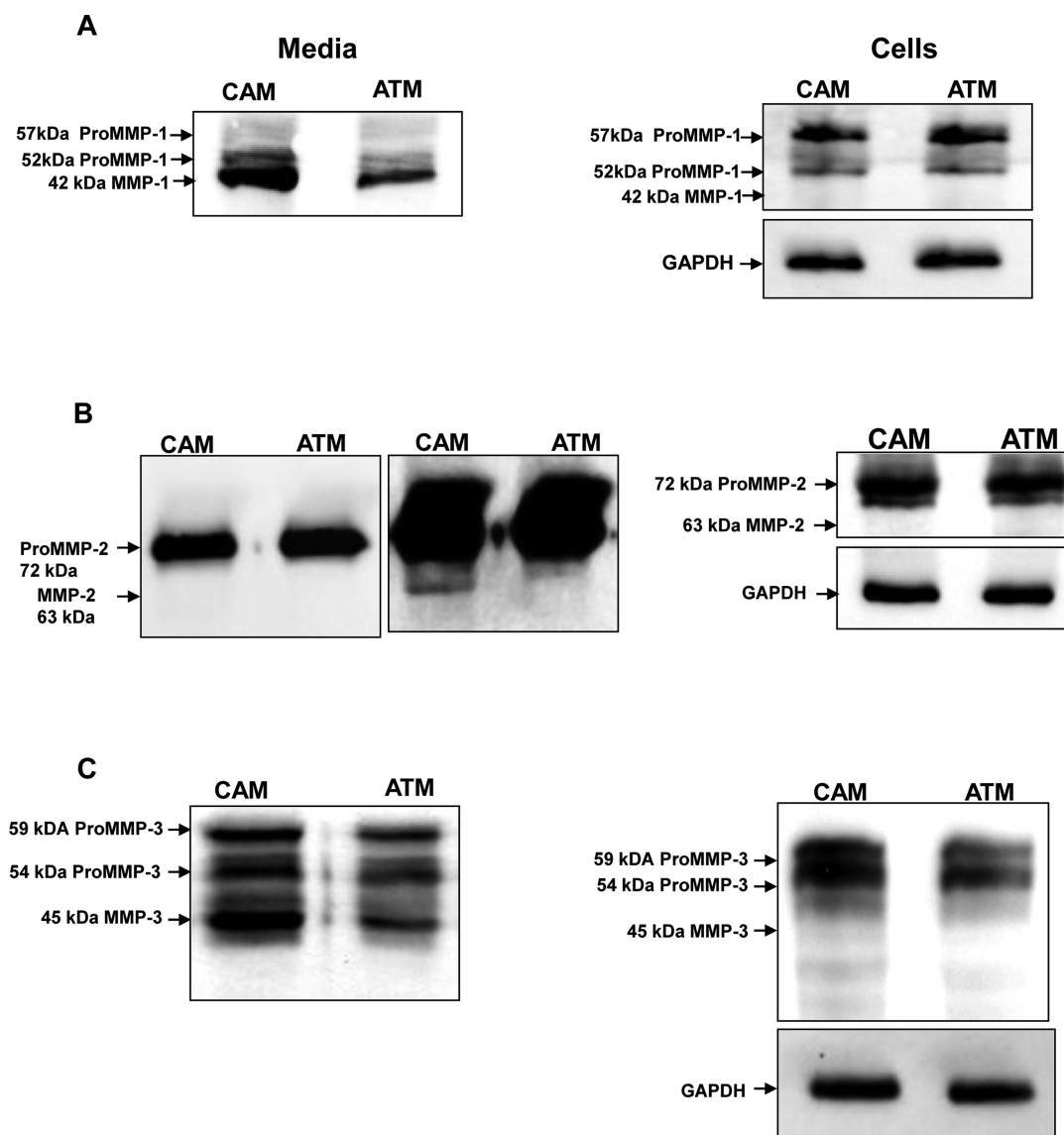
Figure 3. Western blots show the active forms of MMP-1, MMP-2, and MMP-3 in CAM media. (A) Representative Western blots of MMP-1 in CAM and ATM media (left) and cell extracts (right). (B) Representative Western blots of MMP-2 in CAM and ATM media (left) and cell extracts (right). (C) Representative Western blots of MMP-3 in CAM and ATM media at two different exposures (left, center) and cell extracts (right).

corresponded to neo-N-termini in the COFRADIC data set (Supporting Information Table S5). Approximately 50% of all unique proteins identified corresponded to putative secreted proteins (Supporting Information Table S6). In the functional classification, "binding proteins" and "ECM" proteins again predominated (Figure 1B). Furthermore, 41 proteins were identified that were not seen in the first set of SILAC experiments, of which 24 were known extracellular proteins.

CAM-Restricted Proteolytic Events

In the data set as a whole, neo-N-termini corresponding to putative proteolytic cleavage sites were identified in a total of 94 unique proteins, of which collagens alpha1(I) and alpha-2(I) and IGFBP-5 had the most cleavage sites (Supporting Information Table S7). In order to refine cancer-related changes, we then sought those proteins for which unique neo-N-termini were identified in CAM secretomes relative to their ATM counterparts. Applying this criterion, we identified 13 proteins that exhibited CAM-restricted proteolytic cleavage (Table 1): strikingly, these included cleavages in the propeptide

domains of MMP-1 (interstitial collagenase) and MMP-3 (stromelysin-1) (Table 1 and Supporting Information Figure S2); moreover, N-terminal COFRADIC also identified increased prodomain cleavage in MMP-2 (72 kDa type IV collagenase) (Supporting Information Table S7).

In Vivo MMP Activity

To determine the in vivo relevance of myofibroblasts for MMP activity in tumors, we made use of FMT imaging of a MMP fluorescent substrate in a xenograft model consisting of MKN45 gastric cancer cells alone or with human CAMs. In matched tumors of similar size generated with and without coadministration of CAMs, the MMPSense substrate revealed significantly increased activity when human CAMs were present (Figure 2) .

Activation of MMP-1, -2, and -3 in CAM Media

The substrate used for in vivo imaging does not distinguish individual MMPs, and subsequent studies therefore made use of in vitro techniques to assess the relative contribution of
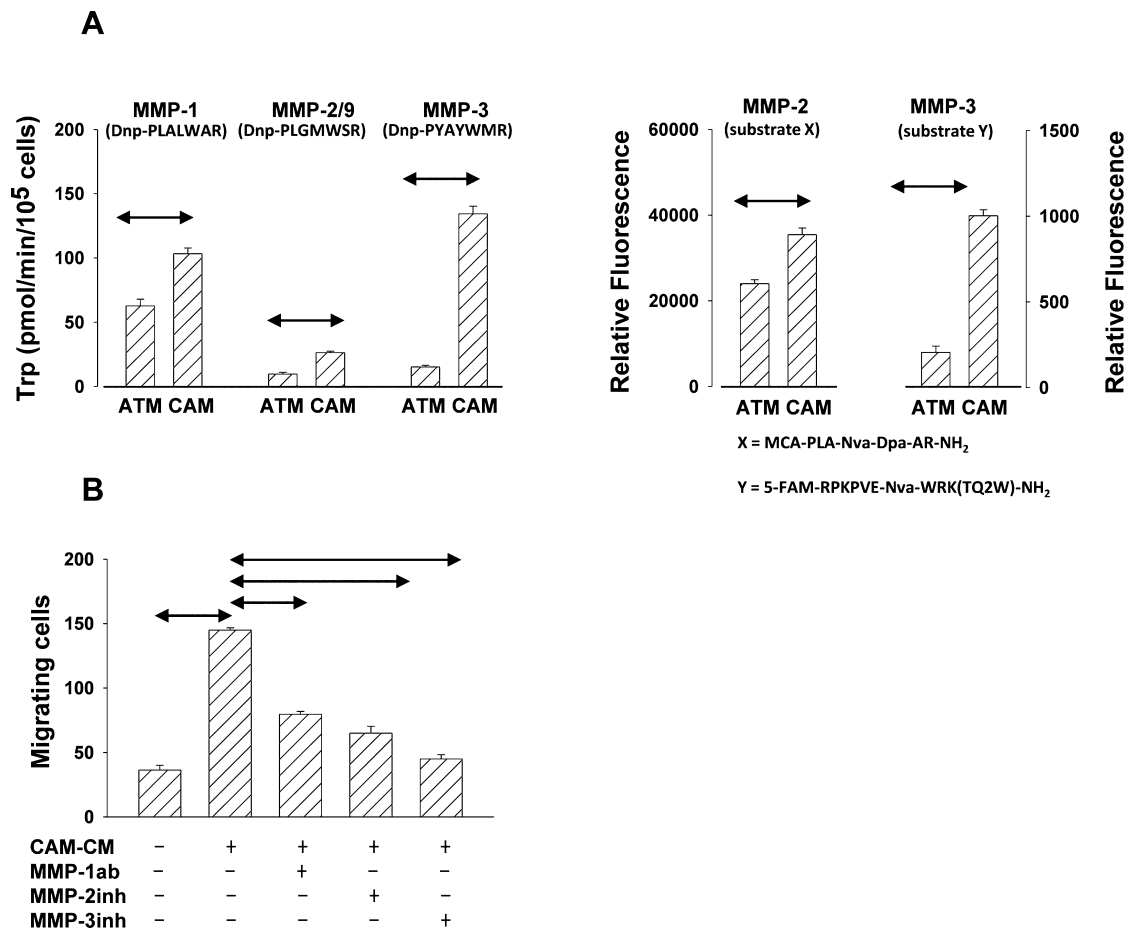
Figure 4. Increased MMP-1, MMP-2, and MMP-3 activity in CAM media. (A) MMP-1, MMP-2, and MMP-3 enzyme activities (using the selective substrates indicated in brackets) are increased in CAM compared with ATM media; left, assays based on Trp fluorescence and right on FRET. (B) CAM-CM media stimulates AGS cell migration and is inhibited by neutralizing antibody to MMP-1 (2.5 μg mL^{-1}) or inhibitors (see text) of MMP-2 (6 μM) and MMP-3 (3 μM). Horizontal bars, $p < 0.05$.

MMPs1−3 in CAM media. Western blots of MMP-1 revealed increased abundance of a 42 kDa form corresponding to the active enzyme in CAM compared with ATM media; in contrast, in cell extracts of the two cell types there was similar abundance of the precursor proteins of 57 and 52 kDa (Figure 3A). For MMP-2, we identified a precursor form of 72 kD in cells and media of both CAMs and ATMs, again in similar abundance in the two cell types. When blots of media were overexposed it was possible to identify a minor band of 63 kDa corresponding to the active enzyme in CAM but not ATM media (Figure 3B). Finally, for MMP-3 we identified precursor proteins of 59 and 54 kDa in cells and media of both CAMs and ATMs; a band of 45 kDa corresponding to the active enzyme was found in media, and the abundance was greater in CAMs compared with ATMs (Figure 3C).

To establish the functional significance of these results, we then studied MMP enzyme activity in CAM and ATM media. Using a fluorogenic substrate for MMP-1, we found significantly greater activity in CAM compared with the corresponding ATM media (Figure 4A). Similarly, substrates selective for MMP-2, or for MMP-2/MMP-9 (Figure 4A), revealed greater activity in CAM than ATM media, and the same pattern was observed with two different MMP-3 substrates (Figure 4A).

Myofibroblast MMPs and Cancer Cell Migration

There is MMP-stimulation of migration of AGS gastric cancer cells in Boyden chambers,[33] and this was then used to test the functional significance of the changes in MMP abundance and activity in CAM media. Conditioned media (CM) from both CAMs and ATMs stimulated AGS cell migration, but the response to the former was significantly greater than to the latter (CAM-CM: 207 $\pm$ 11 cells per field; ATM-CM: 145 $\pm$ 11, $p < 0.05$; control media: 15 $\pm$ 2). Neutralizing antibody to MMP-1 (2.5 μg mL^{-1}) significantly suppressed AGS cell migration in response to CAM-CM (Figure 4B); similarly, previously characterized selective inhibitors of MMP-2 or MMP-3 at concentrations approximately 3-fold above their reported K_i in each case (6 and 3 μM, respectively)[37,38] also inhibited AGS cell migration in response to CAM-CM, indicating that active MMP-2 and MMP-3 released from myobfibroblasts play a role in cancer cell migration (Figure 4B).

■ DISCUSSION

The tumor microenvironment reflects the secretomes of both cancer and stromal cells including myofibroblasts, fibroblasts, pericytes, endothelial cells, inflammatory and immune cells. Crucially, interactions between different secretomes influence cancer cell migration, invasion and metastasis by multiple mechanisms including the activation or inhibition of proteases

with consequences for the proteolytic cleavage of ECM proteins, growth factors, cytokines and chemokines.[15] The secretomes of cancer cells have attracted increasing attention in recent years,[4−9] but little is yet known of stromal cell secretomes. Differences in the secretomes of myofibroblasts recovered from gastric cancers and those recovered from adjacent tissue have been reported recently using iTRAQ.[19] We have now used SILAC and COFRADIC to determine the extent to which proteolysis influenced myofibroblast secretomes in gastric cancer. Our study identified neo-N-termini derived from 94 proteins in CAM secretomes including evidence of cleavage of the prodomains of MMP-1, -2, and -3 leading to increased extracellular proteolytic activity. The data indicate that a distinguishing feature of cancer myofibroblasts is increased expression and increased activation of these MMPs in an autonomous manner in gastric cancer with the potential for promoting cancer progression.

The identification of secreted biomarkers by cancer cells has been a focus of interest for several generations and has been stimulated more recently by the development and refinement of proteomic methods and the prospect of rigorously defining the cancer secretome.[39] Extracellular proteolysis presents additional challenges in defining the relevant secretomes; it is important not least because it underlies multiple mechanisms implicated in cancer progression including angiogenesis, tumor cell migration and invasion. A number of proteomic methods have recently been used to identify neo-N-termini generated in complex samples including COFRADIC[26] and terminal amine isotopic labeling of substrates (TAILS),[40] which has been applied to the identification of substrates of MMP-2 and MMP-9 in fibroblast secretomes.[41,42] Since SILAC has previously been used successfully for secretome studies in a range of cell types including stromal cells from other tissues,[43,44] and since COFRADIC coupled with SILAC labeling is considered to offer a rigorous approach to N-terminomics,[26,42] these methods were selected for the present studies.

The present study identified proteins in media released by the endoplasmic reticulum−Golgi secretory pathway; however, as commonly found in secretome studies, there were also proteins likely to be released by other mechanisms including cytoplasmic proteins liberated through cell death, shedding of membrane proteins and release of exosomes. Previous studies have identified similar rates of apoptosis in CAMs and ATMs[19] suggesting that differential cell death is unlikely to account for differences in the CAM and ATM secretomes. For proteins released through classical secretory mechanisms, we were able to identify many previously reported in the secretomes of fibroblasts and of the stem cells that may give rise to them, including extracellular matrix proteins, IGFBPs, MMPs and TIMPs.[12,44] The differences between CAM and ATM secretomes may reflect alterations in gene expression, post-translational processing, relative rates of secretion and in proteolysis following release. We have now defined the latter though identification of neo-N-termini in CAMs compared with their corresponding ATMs. For example, we found multiple neo-N-termini in collagens alpha-2 (I) and alpha-1(I), and IGFBP5, as well as at limited sites in 91 other proteins. In a small subset of proteins we identified neo-N-termini that were unique to CAMs, and these included six neo-N-termini in the prodomains of MMP-1 and MMP-3, suggesting that activation of these MMPs might be functionally important in CAMs.

It is well established that MMP activity is increased in tumors and promotes cancer cell migration and invasion;[13] the present in vivo imaging data indicate that CAMs contribute to this increased activity in an animal model. It is likely that MMPs have multiple roles in different tumor functions accounting for the fact that MMP inhibitors have not yet led to successful anticancer therapies.[15] The present demonstration of increased expression and activation of MMP-1, MMP-2 and MMP-3 in CAM secretomes nevertheless suggests a novel dimension to the role of these enzymes. In vivo there may be activation of myofibroblast MMPs by epithelial or cancer-derived proteases, e.g., MMP-7.[33] Importantly, however, the present data indicate that increased MMP activity in CAM media occurs independently of a cancer or epithelial cell stimulus. This is nevertheless relevant to cancer cell function not least because MMP-1, MMP-2, and MMP-3 stimulate cancer cell migration and make a substantial contribution to the chemotactic properties of CAM conditioned media. The prodomain cleavages of MMP-1, -2, and -3 identified here are all on the N-terminal side of the conserved cysteine switch sequence, and we think it is possible that these facilitate activation by exposing the site for autolysis much in the same way that trypsin activates MMPs.[45] However, the precise protease(s) responsible for CAM-autonomous prodomain cleavages is presently unclear and should now be investigated. In this context it is worth noting that there was decreased abundance of protease inhibitors, including TIMPs-1, -2, and -3 in one patient (Supporting Information Table S4), which may contribute to increased protease activity.

The present study using SILAC−COFRADIC has provided the most detailed analysis of gastric cancer myofibroblast secretomes to date. It extends previous studies,[19] but in addition, it defines differences in the extracellular degradomes of CAMs and ATMs. At least some of the differences between CAFs or CAMs and their normal tissue counterparts are thought to reflect interactions that occur in the presence of cancer cells.[3] The present data indicate that selective MMP-activation occurs in the CAM secretome even when these cells are cultured in the absence of cancer cells. This property reflects a cell-autonomous mechanism by which CAMs might contribute to a cancer-promoting microenvironment. The possibility of targeting anticancer therapies to stromal cells has emerged recently,[46] and the present data indicate how these could be refined to include the stromal degradome.

■ ASSOCIATED CONTENT

Ⓢ Supporting Information

Supporting methods, tables, and figures. This material is available free of charge via the Internet at http://pubs.acs.org.

■ AUTHOR INFORMATION

Corresponding Author

*Tel: (44)(0)151 794 5331. E-mail: avarro@liverpool.ac.uk.

Notes

The authors declare no competing financial interest.

■ ACKNOWLEDGMENTS

ABBREVIATIONS:

ATM, adjacent tissue myofibroblast; CAM, cancer-associated myofibroblast; COFRADIC, combined fractional diagonal chromatography; IGFBP, insulin-like growth factor binding protein; MMP, matrix metalloproteinase

REFERENCES

(1) Bissell, M. J.; Radisky, D. Putting tumours in context. *Nat. Rev. Cancer* **2001**, *1* (1), 46−54.

(2) Tlsty, T. D.; Coussens, L. M. Tumor stroma and regulation of cancer development. *Annu. Rev. Pathol.* **2006**, *1*, 119−150.

(3) Hanahan, D.; Weinberg, R. A. Hallmarks of cancer: the next generation. *Cell* **2011**, *144* (5), 646−674.

(4) Faca, V. M.; Ventura, A. P.; Fitzgibbon, M. P.; Pereira-Faca, S. R.; Pitteri, S. J.; Green, A. E.; Ireton, R. C.; Zhang, Q.; Wang, H.; O'Briant, K. C.; Drescher, C. W.; Schummer, M.; McIntosh, M. W.; Knudsen, B. S.; Hanash, S. M. Proteomic analysis of ovarian cancer cells reveals dynamic processes of protein secretion and shedding of extra-cellular domains. *PLoS One* **2008**, *3* (6), e2425.

(5) Kulasingam, V.; Diamandis, E. P. Proteomics analysis of conditioned media from three breast cancer cell lines: a mine for biomarkers and therapeutic targets. *Mol. Cell. Proteomics* **2007**, *6* (11), 1997−2011.

(6) Lawlor, K.; Nazarian, A.; Lacomis, L.; Tempst, P.; Villanueva, J. Pathway-based biomarker search by high-throughput proteomics profiling of secretomes. *J. Proteome Res.* **2009**, *8* (3), 1489−1503.

(7) Marimuthu, A.; Subbannayya, Y.; Sahasrabuddhe, N. A.; Balakrishnan, L.; Syed, N.; Sekhar, N. R.; Katte, T. V.; Pinto, S. M.; Srikanth, S. M.; Kumar, P.; Pawar, H.; Kashyap, M. K.; Maharudraiah, J.; Ashktorab, H.; Smoot, D. T.; Ramaswamy, G.; Kumar, R. V.; Cheng, Y.; Meltzer, S. J.; Roa, J. C.; Chaerkady, R.; Prasad, T. S.; Harsha, H. C.; Chatterjee, A.; Pandey, A. SILAC-based quantitative proteomic analysis of gastric cancer secretome. *Proteomics: Clin. Appl.* **2012**, DOI: 10.1002/prca.201200069.

(8) Khwaja, F. W.; Svoboda, P.; Reed, M.; Pohl, J.; Pyrzynska, B.; Van Meir, E. G. Proteomic identification of the wt-p53-regulated tumor cell secretome. *Oncogene* **2006**, *25* (58), 7650−7661.

(9) Volmer, M. W.; Radacz, Y.; Hahn, S. A.; Klein-Scory, S.; Stuhler, K.; Zapatka, M.; Schmiegel, W.; Meyer, H. E.; Schwarte-Waldhoff, I. Tumor suppressor Smad4 mediates downregulation of the anti-adhesive invasion-promoting matricellular protein SPARC: Landscaping activity of Smad4 as revealed by a "secretome" analysis. *Proteomics* **2004**, *4* (5), 1324−1334.

(10) Zhong, L.; Roybal, J.; Chaerkady, R.; Zhang, W.; Choi, K.; Alvarez, C. A.; Tran, H.; Creighton, C. J.; Yan, S.; Strieter, R. M.; Pandey, A.; Kurie, J. M. Identification of secreted proteins that mediate cell-cell interactions in an in vitro model of the lung cancer microenvironment. *Cancer Res.* **2008**, *68* (17), 7237−7245.

(11) De Boeck, A.; Hendrix, A.; Maynard, D.; Van Bockstal, M.; Daniels, A.; Pauwels, P.; Gespach, C.; Bracke, M.; De Wever, O. Differential secretome analysis of cancer-associated fibroblasts and bone marrow-derived precursors to identify microenvironmental regulators of colon cancer progression. *Proteomics* **2013**, *13* (2), 379−388.

(12) Xu, B. J.; Yan, W.; Jovanovic, B.; An, A. Q.; Cheng, N.; Aakre, M. E.; Yi, Y.; Eng, J.; Link, A. J.; Moses, H. L. Quantitative analysis of the secretome of TGF-beta signaling-deficient mammary fibroblasts. *Proteomics* **2010**, *10* (13), 2458−2470.

(13) Egeblad, M.; Werb, Z. New functions for the matrix metalloproteinases in cancer progression. *Nat. Rev. Cancer* **2002**, *2* (3), 161−174.

(14) Lopez-Otin, C.; Matrisian, L. M. Emerging roles of proteases in tumour suppression. *Nat. Rev. Cancer* **2007**, *7* (10), 800−808.

(15) Overall, C. M.; Kleifeld, O. Tumour microenvironment—opinion: validating matrix metalloproteinases as drug targets and antitargets for cancer therapy. *Nat. Rev. Cancer* **2006**, *6* (3), 227−239.

(16) Bhowmick, N. A.; Neilson, E. G.; Moses, H. L. Stromal fibroblasts in cancer initiation and progression. *Nature* **2004**, *432* (7015), 332−337.

(17) Kalluri, R.; Zeisberg, M. Fibroblasts in cancer. *Nat. Rev. Cancer* **2006**, *6* (5), 392−401.

(18) De Wever, O.; Demetter, P.; Mareel, M.; Bracke, M. Stromal myofibroblasts are drivers of invasive cancer growth. *Int. J. Cancer* **2008**, *123* (10), 2229−2238.

(19) Holmberg, C.; Quante, M.; Steele, I.; Kumar, J.; Balabanova, S.; Duval, C.; Czepan, M.; Rakonczayjr, Z.; Tiszlavicz, L.; Nemeth, I.; Lazar, G.; Simonka, Z.; Jenkins, R.; Hegyi, P.; Wang, T.; Dockray, G.; Varro, A. Release of TGFbetaig-h3 by gastric myofibroblasts slows tumor growth and is decreased with cancer progression. *Carcinogenesis* **2012**, *33*, 1553−1562.

(20) Powell, D. W.; Mifflin, R. C.; Valentich, J. D.; Crowe, S. E.; Saada, J. I.; West, A. B. Myofibroblasts. I. Paracrine cells important in health and disease. *Am. J. Physiol.* **1999**, *277* (1 Pt 1), C1−C9.

(21) Powell, D. W.; Pinchuk, I. V.; Saada, J. I.; Chen, X.; Mifflin, R. C. Mesenchymal cells of the intestinal lamina propria. *Annu. Rev. Physiol.* **2011**, *73*, 213−237.

(22) Houghton, J.; Stoicov, C.; Nomura, S.; Rogers, A. B.; Carlson, J.; Li, H.; Cai, X.; Fox, J. G.; Goldenring, J. R.; Wang, T. C. Gastric cancer originating from bone marrow-derived cells. *Science* **2004**, *306* (5701), 1568−1571.

(23) Quante, M.; Tu, S. P.; Tomita, H.; Gonda, T.; Wang, S. S.; Takashi, S.; Baik, G. H.; Shibata, W.; Diprete, B.; Betz, K. S.; Friedman, R.; Varro, A.; Tycko, B.; Wang, T. C. Bone marrow-derived myofibroblasts contribute to the mesenchymal stem cell niche and promote tumor growth. *Cancer Cell* **2011**, *19* (2), 257−272.

(24) Jiang, L.; Gonda, T. A.; Gamble, M. V.; Salas, M.; Seshan, V.; Tu, S.; Twaddell, W. S.; Hegyi, P.; Lazar, G.; Steele, I.; Varro, A.; Wang, T. C.; Tycko, B. Global hypomethylation of genomic DNA in cancer-associated myofibroblasts. *Cancer Res.* **2008**, *68* (23), 9900−9908.

(25) Gevaert, K.; Van Damme, J.; Goethals, M.; Thomas, G. R.; Hoorelbeke, B.; Demol, H.; Martens, L.; Puype, M.; Staes, A.; Vandekerckhove, J. Chromatographic isolation of methionine-containing peptides for gel-free proteome analysis: identification of more than 800 *Escherichia coli* proteins. *Mol. Cell. Proteomics* **2002**, *1* (11), 896−903.

(26) Gevaert, K.; Goethals, M.; Martens, L.; Van, D. J.; Staes, A.; Thomas, G. R.; Vandekerckhove, J. Exploring proteomes and analyzing protein processing by mass spectrometric identification of sorted N-terminal peptides. *Nat. Biotechnol.* **2003**, *21* (5), 566−569.

(27) Staes, A.; Impens, F.; Van Damme, P.; Ruttens, B.; Goethals, M.; Demol, H.; Timmerman, E.; Vandekerckhove, J.; Gevaert, K. Selecting protein N-terminal peptides by combined fractional diagonal chromatography. *Nat. Protoc.* **2011**, *6* (8), 1130−1141.

(28) Ghesquiere, B.; Colaert, N.; Helsens, K.; Dejager, L.; Vanhaute, C.; Verleysen, K.; Kas, K.; Timmerman, E.; Goethals, M.; Libert, C.; Vandekerckhove, J.; Gevaert, K. In vitro and in vivo protein-bound tyrosine nitration characterized by diagonal chromatography. *Mol. Cell. Proteomics* **2009**, *8* (12), 2642−2652.

(29) Impens, F.; Colaert, N.; Helsens, K.; Ghesquiere, B.; Timmerman, E.; De Bock, P. J.; Chain, B. M.; Vandekerckhove, J.; Gevaert, K. A quantitative proteomics design for systematic identification of protease cleavage events. *Mol. Cell. Proteomics* **2010**, *9* (10), 2327−2333.

(30) Helsens, K.; Colaert, N.; Barsnes, H.; Muth, T.; Flikka, K.; Staes, A.; Timmerman, E.; Wortelkamp, S.; Sickmann, A.; Vandekerckhove, J.; Gevaert, K.; Martens, L. ms_lims, a simple yet powerful open source laboratory information management system for MS-driven proteomics. *Proteomics* **2010**, *10* (6), 1261−1264.

(31) Colaert, N.; Helsens, K.; Impens, F.; Vandekerckhove, J.; Gevaert, K. Rover: a tool to visualize and validate quantitative proteomics data from different sources. *Proteomics* **2010**, *10* (6), 1226−1229.

(32) Barsnes, H.; Vizcaino, J. A.; Eidhammer, I.; Martens, L. PRIDE Converter: making proteomics data-sharing easy. *Nat. Biotechnol.* **2009**, *27* (7), 598−599.

(33) Hemers, E.; Duval, C.; McCaig, C.; Handley, M.; Dockray, G. J.; Varro, A. Insulin-like growth factor binding protein-5 is a target of matrix metalloproteinase-7: implications for epithelial-mesenchymal signaling. *Cancer Res.* **2005**, *65* (16), 7363−7369.

(34) Netzel-Arnett, S.; Fields, G. B.; Birkedal-Hansen, H.; Van Wart, H. E. Sequence specificities of human fibroblast and neutrophil collagenases. *J. Biol. Chem.* **1991**, *266* (11), 6747−6755.

(35) McCaig, C.; Duval, C.; Hemers, E.; Steele, I.; Pritchard, D. M.; Przemeck, S.; Dimaline, R.; Ahmed, S.; Bodger, K.; Kerrigan, D. D.; Wang, T. C.; Dockray, G. J.; Varro, A. The role of matrix metalloproteinase-7 in redefining the gastric microenvironment in response to *Helicobacter pylori*. *Gastroenterology* **2006**, *130* (6), 1754−1763.

(36) Varro, A.; Noble, P. J.; Pritchard, D. M.; Kennedy, S.; Hart, C. A.; Dimaline, R.; Dockray, G. J. *Helicobacter pylori* induces plasminogen activator inhibitor 2 (PAI-2) in gastric epithelial cells through NF-kB and RhoA: implications for invasion and apoptosis. *Cancer Res.* **2004**, *64*, 1695−1702.

(37) Jacobsen, E. J.; Mitchell, M. A.; Hendges, S. K.; Belonga, K. L.; Skaletzky, L. L.; Stelzer, L. S.; Lindberg, T. J.; Fritzen, E. L.; Schostarez, H. J.; O'Sullivan, T. J.; Maggiora, L. L.; Stuchly, C. W.; Laborde, A. L.; Kubicek, M. F.; Poorman, R. A.; Beck, J. M.; Miller, H. R.; Petzold, G. L.; Scott, P. S.; Truesdell, S. E.; Wallace, T. L.; Wilks, J. W.; Fisher, C.; Goodman, L. V.; Kaytes, P. S.; et al. Synthesis of a series of stromelysin-selective thiadiazole urea matrix metalloproteinase inhibitors. *J. Med. Chem.* **1999**, *42* (9), 1525−1536.

(38) Koivunen, E.; Arap, W.; Valtanen, H.; Rainisalo, A.; Medina, O. P.; Heikkila, P.; Kantor, C.; Gahmberg, C. G.; Salo, T.; Konttinen, Y. T.; Sorsa, T.; Ruoslahti, E.; Pasqualini, R. Tumor targeting with a selective gelatinase inhibitor. *Nat. Biotechnol.* **1999**, *17* (8), 768−774.

(39) Hanash, S.; Taguchi, A. The grand challenge to decipher the cancer proteome. *Nat. Rev. Cancer* **2010**, *10* (9), 652−660.

(40) Kleifeld, O.; Doucet, A.; auf dem Keller, U.; Prudova, A.; Schilling, O.; Kainthan, R. K.; Starr, A. E.; Foster, L. J.; Kizhakkedathu, J. N.; Overall, C. M. Isotopic labeling of terminal amines in complex samples identifies protein N-termini and protease cleavage products. *Nat. Biotechnol.* **2010**, *28* (3), 281−288.

(41) Dean, R. A.; Overall, C. M. Proteomics discovery of metalloproteinase substrates in the cellular context by iTRAQ labeling reveals a diverse MMP-2 substrate degradome. *Mol. Cell. Proteomics* **2007**, *6* (4), 611−623.

(42) Prudova, A.; auf dem, K. U.; Butler, G. S.; Overall, C. M. Multiplex N-terminome analysis of MMP-2 and MMP-9 substrate degradomes by iTRAQ-TAILS quantitative proteomics. *Mol. Cell. Proteomics* **2010**, *9* (5), 894−911.

(43) Dowling, P.; Clynes, M. Conditioned media from cell lines: a complementary model to clinical specimens for the discovery of disease-specific biomarkers. *Proteomics* **2011**, *11* (4), 794−804.

(44) Skalnikova, H.; Motlik, J.; Gadher, S. J.; Kovarova, H. Mapping of the secretome of primary isolates of mammalian cells, stem cells and derived cell lines. *Proteomics* **2011**, *11* (4), 691−708.

(45) Van Wart, H. E.; Birkedal-Hansen, H. The cysteine switch: a principle of regulation of metalloproteinase activity with potential applicability to the entire matrix metalloproteinase gene family. *Proc. Natl. Acad. Sci. U. S. A.* **1990**, *87* (14), 5578−5582.

(46) Anton, K.; Glod, J. Targeting the tumor stroma in cancer therapy. *Curr. Pharm. Biotechnol.* **2009**, *10* (2), 185−191.